Vol.67: e24240155, 2024
https://doi.org/10.1590/1678-4324-2024240155
ISSN 1678-4324 Online Edition

BABT
Brazilian Archives of Biology and Technology

Article - Engineering, Technology and Techniques

Allocation of Energy Storage Systems in a Hydro-Thermal-Wind System

Alvaro Augusto Waldrigues de Almeida[1,2*]
https://orcid.org/0009-0004-8371-6123

Thelma Solange Piazza Fernandes[1]
https://orcid.org/0000-0002-5167-1547

[1]Universidade Federal do Paraná, Departamento de Engenharia Elétrica, Curitiba, Paraná, Brasil; [2]Universidade Tecnológica Federal do Paraná, Departamento de Eletrotécnica, Curitiba, Paraná, Brasil

Editor-in-Chief: Alexandre Rasi Aoki
Associate Editor: Alexandre Rasi Aoki

Received: 18-Feb-2024; Accepted: 02-Apr-2024

*Correspondence: alvaroaugusto@utfpr.edu.br; Tel.: +55-41-992576549 (A. A. W. A.).

HIGHLIGHTS

- Allocation of large-scale Energy Storage Systems (ESS)
- Genetic Algorithm (GA) and Linear Multi-Period Optimal Power Flow (LMOPF)
- High-Voltage Hydro-Thermal-Wind System, 408 buses, used to test the model
- Marginal Operating Costs used to configure allocation cases

Abstract: Strong concerns over greenhouse gas emissions have required the construction of non-polluting energy sources such as wind farms and photovoltaic plants. This need, combined with recent technological developments, has enabled the global installed capacity of wind farms in particular to grow from a negligible level in 2001 to more than 900 GW in 2023. However, due to the high variability of wind, this energy source is non-dispatchable, *i.e.*, it cannot be controlled by operators to meet demand in a short amount of time. This problem can be mitigated by the allocation of energy storage systems (ESSs) to appropriate buses. This paper proposes an optimization model for the allocation of large-scale ESSs using a genetic algorithm (GA) and a linear multi-period optimal power flow (LMOPF). The GA enables the best allocation of the ESS to buses, their dimensions (*i.e.*, selection of the power and energy of the ESS) and four types of technology. The LMOPF is used to perform system planning for a horizon of np periods, and to carry out the generation dispatch of a high voltage hydro-thermal-wind system and the charging and discharging processes of the ESS allocated by the GA. Due to the large size of the system and the complexity of resolution, a single-phase network model was chosen, and reactive power was disregarded. The model was tested using a system in the south of Brazil. The results showed that the optimal allocation of ESSs allowed for a hydroelectric energy time-shift, reducing the daily costs of operation.

Keywords: Allocation of energy storage systems; arbitrage; energy time-shift; genetic algorithms; linear multi-period optimal power flow.

INTRODUCTION

The first large-scale ESS (energy storage system) was a PHES (pumped hydro energy storage), constructed in Italy and Switzerland in 1890. Since then, many other technologies have been developed, and ESSs have found many applications in the areas of generation and transmission, such as [1-7]:

- Grid integration of wind and photovoltaic generation. There has been a huge increase in the use of these sources worldwide since 2001. However, they are non-dispatchable. The allocation of ESSs to appropriate system buses has the potential to mitigate this problem;
- Electric energy time-shift (a phenomenon also known as arbitrage), where cheap energy is bought during an off-peak period, stored, and sold at a better price during a later peak period;
- Electric supply capacity, which reduces the need for new generating plants and the purchase of energy on the wholesale market;
- Energy storage during periods of favorable hydrological conditions;
- Transmission congestion relief, to postpone investment in new lines;
- Reduction of operating costs of transmission systems;
- Suppression of demand peaks;
- Ancillary services, such as frequency regulation, spinning and non-spinning reserves, voltage support and black start.

For all ESS applications, it is important to allocate and size the most appropriate storage technologies. The question of the allocation of ESSs has been addressed by several authors using various techniques. The list below shows some works related to the use of some of these techniques. The authors consider only battery energy storage systems (BESSs) and low voltage (LV) or medium voltage (MV) distribution systems (DSs).

Awad, El-Fouly, and Salama [8] studied the problem of optimizing a combination of BESSs and loads for a DS, so that all possible contingencies could be met. A GA (Genetic Algorithm) was used to build a model, which was tested using a system containing two BESSs and 16 buses, and a system containing two BESSs and 32 buses.

Babacan, Torre, and Kleissl [9] studied the allocation of BESSs in MV (7.2 kV) and LV (120/240 V) systems and with high photovoltaic (PV) penetration (50%). A case study was conducted using a GA and OpenDSS, with the IEEE-8500 system bus.

Awad, EL-Fouly, and Salama [10] proposed a methodology based on the GA and a linear-programming solver. The DS contained 33 buses and three different types of BESS technologies. Two different types of DG were considered, based on natural gas and intermittent wind power.

Rangel and coauthors [11] used a GA with a nonlinear optimization model to determine the allocation of one or more BESSs, and established the type, capacity, location bus and number of elements to be used. The methodology was tested using an IEEE-123 system bus.

Mazza and coauthors [12] presented an approach for planning and scheduling BESSs in an LV system that combined the properties of metaheuristics for BESS sizing and placement with a GA and a greedy algorithm to find the optimal BESS schedule.

Wong and Ramachandaramurthy [13] used WOA to minimize the total system losses by finding the optimal BESS locations and sizing. The DS consisted of 48 buses operating in an MV network. The authors compared the performances of WOA, Particle Swarm Optimization (PSO) and Firefly Algorithm (FA) and concluded that WOA provided the highest overall reduction in system losses.

Most of the literature presents models that allocate and size only BESSs operating in Medium Voltage Thermal-Wind System. However, the distinguishing feature of the present work is the proposition of an optimization model that:

- Allocates not only BESSs, but also pumped hydro energy storage (PHESs), liquid air energy storage (LAESs), and gravity energy storage system (GESSs). To do so, the model uses different values of cost, cycle efficiency, lifetime, discharge times and physical restrictions relative to each technology analyzed;
- Focuses on the electric energy time-shifting properties of the ESSs of a High Voltage (HV) Hydro-Thermal-Wind System with a strong predominance of hydroelectric power (like the Brazilian power system);
- Considers the profitability of arbitration as an allocation criterion, i.e., the allocation of ESSs is only considered viable in the case of a positive net result. This criterion also makes the model more real and closer to a practical commercial situation.

To achieve this, the present work proposes a method for solving an optimization problem that can determine the best buses on which to allocate ESSs, the best ESS technology, and the best dimensions for these, with the aim of minimizing the daily operating costs of the system in study. Four of these technologies were considered for the purpose of this paper, as described below.

Pumped Hydro Energy Storage (PHES)

PHESs can work either in pumping mode, where an electric motor pumps water from a lower reservoir to an upper reservoir, or in generation mode, where water from an upper reservoir is discharged to a lower reservoir through a penstock. The water causes rotation of the pump turbines, which start to operate in turbine mode, activating the generators.

The worldwide installed capacity of PHESs was 183,896 MW in 2023, corresponding to more than 95% of the total number of ESSs [14]. In the USA, Germany and Japan, the construction of hourly cycle PHESs began to increase from the 1960s onwards in order to supply energy at peak hours. The current interest in PHESs and other ESS technologies is mainly due to the need to reduce the intermittency of wind and solar power plants. China is one of the leading countries in terms of the construction of new PHESs [15]. In Brazil, an inventory study was carried out by the Energy Research Office (EPE) [16], but there are still no PHESs operating or under construction in this country.

The size of the reservoir generally determines the level of the charging and discharging cycle for PHESs, which may be hourly, daily, weekly, monthly, or seasonal. Although PHES can offer a large capacity, the major constraint is of a geological nature, and is associated with the need to build reservoirs, increasing Capex (capital expenditure), and especially Capex power.

Battery Energy Storage System (BESS)

BESSs are electrochemical ESSs that produce and store energy through oxidation and reduction processes. BESSs do not suffer from major geological constraints, except those arising from logistical factors, in the same way as all ESSs. However, a major constraint is their reduced lifetime compared to other ESSs, which is due to degradation mechanisms [17].

BESSs are becoming cheaper and more efficient, with higher sizes (MW/MWh), and have been installed in several countries. Up to the moment when this paper was submitted, the highest operational BESS in the world was Moss Landing, 750 MW/3,000 MWh, California, USA [18]. In Brazil, this subject has been under discussion since 2019, and the company ISA CTEEP installed a 30 MW/60 MWh BESS in the locality of Registro, SP, in March 2023 [19]. The construction of higher BESSs is expected in Brazil in the coming years [20]. BESSs show a great range of technological diversity [7, 21]. However, this diversity is not considered in the present paper.

Liquid Air Energy Storage (LAES)

In LAES, the ambient air is purified, compressed, and cooled until it reaches the liquid phase, when it is stored in reservoirs at almost atmospheric pressure [22]. During discharge, energy is recovered by pumping, evaporating, and expanding the liquid air through a set of turbines, which drive electric generators. A pilot plant based on this technology, with power of 350 kW/2.5 MWh, was commissioned in 2010 as a result of a joint effort by Highview Power and the University of Leeds, UK. A new 5 MW/15 MWh plant, built near Manchester, UK, was commissioned in 2018 and connected to the system. Highview Power reports that the company also have LAES projects under development in Scotland and Australia [23]. Despite being a recent technology in relation to BESSs, LAESs have a significant advantage, which is the impossibility of degradation.

Gravity Energy Storage System (GESS)

GESS operates by storing gravitational potential energy, in the same way as PHES. However, in PHES, potential energy is increased by pumping water to an upper reservoir, whereas in GESS this increase takes place through the vertical or inclined movement of large solid blocks [24, 25].

Like BESSs and LAESs, GESSs do not suffer from the geological constraints, and like PHESs and LAESs, GESSs are immune to degradation. In addition, although this technology is still recent, the Capex of a GESS may be lower than for the other technologies. GESS technology is not yet in the commercial phase, but it has attracted increasing attention. In 2010, there were five patents, whereas this number had increased to 46 by 2021, when the technology began to attract attention. Energy Vault, a Swiss-based company, initiated the commissioning process of a 25 MW/100 MWh GESS in Roding, China, in December 2023 [26].

Parameters adopted in this study

The parameters used for the present study are shown in Table 1 [7, 27-33]. A parameter of special importance, which was considered in the present paper, is the location adaptability: whereas BESSs, LAESs and GESSs can be allocated to any bus of the system under study, PHES can only be allocated to buses close to rivers. In the present paper, logistical factors were not considered, and inventory studies related to PHESs were not carried out.

In what follows, the symbol $ means U.S. Dollars (USD). In the case of marginal operating costs (MCs), the conversion of values from Brazilian Reais (BRL) to USD was carried out based on the average exchange data of 2023. According to the Brazilian Central Bank: 1.0 USD = 5.00 BRL.

Table 1. Parameter values used in the present study

Item	PHES	BESS	LAES	GESS
Power range (MW)	10.0–7,000	1.0–800	1.0–300	40.0–3,000
Location adaptability	Poor	Good	Good	Good
Cycle efficiency	85%	95%	70%	90%
Discharge time (h)	1.5–5 h	1.5–5 h	1.5–5 h	1.5–5 h
Lifetime (years)	50	15	30	40
Capex Energy ($/kWh)	400	100	600	300
Capex Power ($/kW)	5,000	150	2,520	690

MATERIAL AND METHODS

The methodology adopted in the present work involves the development of a model for the allocation of different ESS technologies, with the aim of addressing issues related to the allocation, costs and electric energy time-shift of large high voltage hydro-thermal-wind systems, such as those found in Brazil, with a high hydroelectric capacity and growing wind capacity. In the present paper, ESSs are assumed to operate with constant voltages and frequencies. The optimal allocation is obtained based on the variation in both these prices and wind energy generation.

The maximum number of ESSs to be allocated, the wind daily generation, and the electrical system parameters are input variables. The results are the optimal allocation configuration, which specifies how many ESSs are actually allocated, the types of ESSs allocated to each bus, and other energy and financial results.

Due to the large size of the system, the Linprog function with Interior Point Methods from Matlab® was used. The GA Matlab® toolbox was used to solve the GA problem.

In this work, the allocation of ESSs is carried out by means of an optimization problem whose criterion is the investment amortization period. This period is calculated based on the net result generated by the decrease in the daily operating cost after the allocation of the ESSs. The net result is obtained from the daily operating costs of hydroelectric power plants (HPPs) and thermoelectric power plants (TPPs), the daily cost of load shedding, the depreciation time and the ESSs acquisition costs. To obtain the daily optimization costs, it is necessary to consider the operation of the system, including the dispatch of HPPs and TPPs, charging and discharging of the ESSs, and load shedding.

The problem is solved on two steps: (1) formulation of the evaluation function; (2) formulation of the LMOPF, which is used to calculate the evaluation function.

Optimization variables are defined at the first step. They are the locations of the buses to which the ESS will be allocated, the dimensions (*i.e.*, the power and energy of the ESS) and the ESS technology used (BESS, PHES, LAES or GESS). These are modeled as binary variables, and are optimized by minimizing the amortization time function using a GA. A GA was chosen due to its ease of implementation and because this is a well-established technique for allocation problems. Many other techniques could be used, such as a particle swarm or differential evolution technique, among others.

At the second step, each individual generated by the GA is evaluated, based on a linear multi-period optimal power flow (LMOPF), which enables the operation of the system. The LMOPF uses linear equations for the power flow corresponding to the active power balances of the network, to satisfy the energy goals of HPPs, the operational limits on the power of HPPs and TPPs, the operational limits on the power and energy of the ESS, and the limits on the active power flows through the lines of the network.

Linear equations were used to model the transmission network due to the size of the problem, which would involve very long computational times if nonlinear equations were used.

The LMOPF performs system planning for a horizon of np periods ahead of a selected planning horizon and optimizes the power grid simultaneously for all of these np periods. If the study horizon is one day, np is equal to 24, and each period lasts one hour ($\Delta t = 1$).

The LMOPF formulation presented in this paper was inspired by a nonlinear formulation that was applied to distribution networks in order to minimize the electrical losses [34]. This formulation was adapted to include the energy constraints of HPPs and the minimization of load shedding that may be necessary to overcome line congestion problems.

Formulation of the evaluation function

Some parameters needed to the formulation of this function are described in Table 2 bellow.

Table 2. System parameters

Type	Description
nb	Number of buses of the system
nl	Number of lines of the system
nld	Number of loads
nh	Number of hydroelectric power plants (HPP)
nt	Number of thermoelectric power plants (TPP)
nw	Number of wind power plants (WF)
np	Number of periods
nsd	Number of ESSs
$costsESS$	ESSs costs (from Table 1) ($/kWh)
MC_{level}^{t}	Marginal operating cost of each period t in a given load level ($/MWh)
LSC_{level}^{t}	Load shedding cost of each period t in a given load level (pu)

At the first step of the optimization problem, the following evaluation function is used to size and allocate the ESSs:

$$fitness = YearsAmortize, \tag{1}$$

where $YearsAmortize$ refers to the amortization time of the investments needed to allocate ESSs.

To obtain the value of $YearsAmortize$, it is necessary to calculate the daily cost of operation before and after storage allocation, as follows:

$$DailyCost_{withoutESS} = \left\{\sum_{t=1}^{np}\sum_{j=1}^{nb} ct\left(PGT_j^t\right) + \sum_{t=1}^{np}\sum_{j=1}^{nb} ch\left(PGH_j^t\right) + \sum_{t=1}^{np}\sum_{j=1}^{nb} cfic\left(Pfic_j^t\right)\right\}_{withoutESS}, \tag{2}$$

and

$$DailyCost_{withESS} = \left\{\sum_{t=1}^{np}\sum_{j=1}^{nb} ct\left(PGT_j^t\right) + \sum_{t=1}^{np}\sum_{j=1}^{nb} ch\left(PGH_j^t\right) + \sum_{t=1}^{np}\sum_{j=1}^{nb} cfic\left(Pfic_j^t\right)\right\}_{withESS} + \\ + \sum_{k=1}^{nsd} DailyESSCost^k\ , \tag{3}$$

where $DiaryCost_{withoutESS}$ is the daily operating cost without storage allocation;$DiaryCost_{withESS}$ is the daily operating cost with storage allocation; $DailyESSCost$ is the ESS daily cost; np is number of periods; nb is the number of buses; and nsd is the number of ESSs.

The function $ct\left(PGT_j^t\right)$ represents the cost of thermoelectric generation, PGT_j^t is the value of thermoelectric generation at bus j in period t, $ch\left(PGH_j^t\right)$ is the cost of hydroelectric generation, PGH_j^t is the value of hydroelectric generation at bus j in period t, $cfic\left(Pfic_j^t\right)$ is the cost of load shedding, and $Pfic_j^t$ is the load shedding value at bus j in period t. The values PGH_j^t, PGT_j^t and $Pfic_j^t$ are calculated by the LMOPF.

The daily net result obtained after allocating the ESS is:

$$Net\_result = DailyCost_{withoutESSs} - DailyCost_{withESSs}\ , \tag{4}$$

and

$$YearsAmortize = Total\_Acquisition\_ESS/(Net\_result * 365)\ , \tag{5}$$

where $Total\_Acquisition\_ESS$ corresponds to the total acquisition cost of all ESSs.

The evaluation function ($fitness$) is calculated for each of the individuals generated by the GA. The GA is based on a search mechanism where the fittest individuals survive and each possible solution to the problem is represented as a chromosome [35]. To find the best solutions to the problem, a reproduction mechanism is

applied to each generation based on an evolutionary process in which the genetic operators of mutation and crossover, among others, are applied to the genetic material of the chromosome.

The coding template for each ESS to be allocated is divided into three parts. The first gene of the template represents the bus of the location where the ESS would be allocated. It is formed from a binary sequence of $nbits_{\text{buses}}$; once converted to decimal, this sequence represents a position in the vector of candidate buses for the allocation of ESS (with separate allocation vectors for each ESS technology). The number of bits for the first gene depends on the size of the array of candidate buses for storage allocation. If the first gene contains a binary sequence that is decoded to give a number greater than the size of the vector of candidate buses for allocation, that individual is discarded. Parameterizations were made to define the ideal number of generations and individuals. In the case of generations, simulations were carried out considering 1000 to 5000 generations (with steps of 1000 generations), and it was found that beyond 4000 generations no significant gains in fitness were obtained. The same was done with the number of individuals: varying it from 10 to 20 (with steps of 5 individuals), it was found that the ideal number was 15.

The second gene of the template determines the size of the ESS, and is formed of a binary sequence of $nbits_{dim}$. When converted to decimal, this representes a position in the vector of ESS dimensions, where the cost values of Capex energy was assumed to be 200 $/kWh (it is common business practice to use only the Capex energy to measure the costs of the ESSs, which was also adopted in the present work to facilitate computations [6, 32]). In Table 3 below, which shows eight sizing possibilities, the number $nbits_{dim}$ is equal to 3.

The third gene of the template represents the ESS technology to be allocated. As there are four types of technology (BESS, PHES, LAES and GESS), 2 bits are needed to represent these possibilities.

Thus, for each decoded ESS, there are ($nbits_{dim} + nbits_{\text{buses}} + 2$) bits, where the total number of bits is $(nbits_{dim} + nbits\_\text{buses}) * nsd$.

After creating the individuals for each generation, they are decoded, and the dimensions, locations and technologies of each ESS are found to be allocated to selected buses of the system. Each configuration of an allocation is simulated by the LMOPF, which is responsible for the operation of the system used to calculate the evaluation function, as shown in Equation (1).

Table 3. Sizing and costs for ESSs

Power (MW)	Energy (MWh)	Acquisition Cost ($)	Cost/cycle ($)	Time Charge/Discharge (Ƶ) (h)
20	100	1*Capex	1*CAP_cycle	5
50	200	2*Capex	2*CAP_cycle	4
100	400	4*Capex	4*CAP_cycle	4
150	600	6*Capex	6*CAP_cycle	4
200	800	8*Capex	8*CAP_cycle	4
500	1,000	10*Capex	10*CAP_cycle	2
800	1,200	12*Capex	12*CAP_cycle	1.5
1000	1,500	15*Capex	15*CAP_cycle	1.5

Table 4 shows the Capex, the Cap_cycle, and the lifetime used in this paper to obtain the acquisition and the daily operating costs for each type of ESS. The Opex (operating expense) is carried out using the cycle efficiency (Table 1), which is included in the cost/cycle.

Table 4. Factors used in this paper to obtain acquisition and daily operating costs

Item	PHES	BESS	LAES	GESS
Capex ($/kWh)	400	100	600	300
CAP_cycle ($)	2,191.80	1,826.50	5,479.50	2,054.80
Lifetime (years)	50	15	30	40

Formulation of the LMOPF

At the second step of the optimization problem, the generation dispatch is calculated and the charging and discharging processes of the ESS are allocated by decoded each individual solution from the GA. This process is conduct by means of a LMOPF.

Table 5 shows the operational limits of the ESS, Table 6 shows the input variables, and Table 7 shows the optimization variables.

Table 5. Operational limits of the ESS

Type	Description
PGH_j^{min}, PGH_j^{max}	Maximum and minimum limits of hydroelectric active power generation at bus j (pu)
PGT_k^{min}, PGT_k^{max}	Maximum and minimum limits of thermoelectric active power generation at bus k (pu)
F_m^{max}	Maximum limits of active power flow through the line m (pu)
PSA_ℓ^{max}	Maximum power injection limits of ESSs at bus ℓ (which depends on the size of the allocated ESS) (pu)
ESA_ℓ^{max}	Maximum limit of stored energy by the ESS at bus ℓ (which depends on the dimension of the allocated ESS) (puh)
$ESA_\ell^{max}\ to\ period\ 24$	$0.4\ \times ESA_\ell^{max}$ (puh)

Table 6. Input variables for each period t

Type	Description
EH_i^{day}	Daily energy targets for hydroelectric power plants connected at bus i (puh)
PGW_m^t	Hourly wind generation values of the system's wind connected at buses m (pu)
Pd_i^t	Hourly active load values, distributed throughout the day and among all load buses (pu)
ESA_{cheg_ℓ}	Energy pre-stored in ESS_ℓ (set as 40% of the storage capacity of the ESS_ℓ) (puh)
τ_ℓ	Time (hours) for full charge and discharge of the ESS_ℓ (that depends on the choice of allocated ESS, Table 4)

Table 7. Optimization variables for each period *t*

Type	Description
PGH_j^t	Hydroelectric active power generation at bus j, during the period t (pu)
PGT_j^t	Thermoelectric active power generation at bus j, during the period t (pu)
PGW_j^t	Wind generation at bus j, during the period t (pu)
$Pfic_j^t$	Load Shedding at bus j during the period t (pu)
P_j^t	Power injection at bus j during the period t (pu)
θ_i^t	Bus angle i, during the period t (rad)
PSA_j^t	Active power injection of the *ESS* at bus j during the period t (pu)
ESA_j^t	Energy stored by ESA_j at bus j during the period t (puh)
Fl_k^t	Active power flow through the line k during the period t (pu)

Equality Constraints

The power balance for each period and each bus of the system is:

$$P_j^t = (PGH_j^t + PGT_j^t + PGW_j^t + Pfic_j^t) - Pd_j^t \ - PSA_j^t \tag{6}$$

where $j = 1, \dots, nb$ and $t = 1, \dots, np$.

A positive value for PSA_j^t means that ESS *j* is being charged in period *t* (*i.e.*, the bus is absorbing power from the network). A negative value means that the storage system is being discharged (*i.e.*, the bus is injecting power into the network).

The power injection vector is represented by the vector $\boldsymbol{P}^t$ for each block of *nb* equations, referring to each period *t*, and is represented by the expression:

$$\boldsymbol{P}^t = \boldsymbol{B}' \cdot \begin{bmatrix} \theta_i^t \\ \dots \\ \theta_{nb-1}^t \end{bmatrix}, \qquad t = 1, \dots, np \tag{7}$$

where $\boldsymbol{B'}$ is the inductive susceptance matrix, which is reduced by removing the column corresponding to the reference bus.

The equality constraints refer to each active power balance equation per bus and per period, and are expressed as:

$$PG_j^t - Pd_j^t = P_j^t(\theta_i^t), \tag{8}$$

where $j = 1, \ldots, nb$ and $t = 1, \ldots, np$.

The stored energy at each period *k* at bus *i* (ESA_i^k) is the sum of the pre-stored energy, ESA_{arrivg_i}, plus the sum of the stored energy from all periods before period k and the energy in the current period k. This is given by the following equation:

$$ESA_\ell^k = ESA_{arrived_\ell} + \sum_t^{k-1} \left(PSA_\ell^t\right) \Delta t + \left(PSA_\ell^k\right) \Delta t, \tag{9}$$

where t = 1,…, k – 1; ℓ = 1,…, nsd, and Δt is the chosen time interval (in this study, Δt = 1 h).

Inequality Constraints

The operational limits on the HPPs, TPPs, ESS, load shedding and flows though the lines are expressed as the following inequality constraints:

$$PGH_j^{min} \leq PGH_j^t \leq PGH_j^{max} \tag{10}$$

$$PGT_k^{min} \leq PGT_k^t \leq PGT_k^{max} \tag{11}$$

$$0 \leq Pfic_n^t \leq Pd_n^t \tag{12}$$

$$-F_m^{max} \leq Fl_m^t \leq F_m^{max}, \tag{13}$$

where $j = 1, \ldots, nh$; $k = 1, \ldots, nt$; $n = 1, \ldots, nb$; $m = 1, \ldots, nl$; $t = 1, \ldots, np$.

Each hydroelectric plant *j* is unable to dispatch more energy than its forecast reserves for the day ahead, EH_j^{day}, which is obtained from medium-term and short-term planning studies.

Equation (14) is used to monitor the energy goal of each hydroelectric plant:

$$\sum_{t=1}^{np} 24 \times PGH_j^t \leq EH_j^{day}, \tag{14}$$

where $j = 1, \ldots, nh$ and $t = 1, \ldots, np$.

The operational limits on the power and energy of the ESS are represented in Equations (15) and (16), respectively:

$$-PSA_\ell^{max} \leq PSA_\ell^t \leq PSA_\ell^{max} \tag{15}$$

$$0.1 \times ESA_\ell^{max} \leq ESA_\ell^t \leq ESA_\ell^{max}, \tag{16}$$

where $\ell = 1, \ldots, nsd$; $t = 1, \ldots, np$.

The charging and discharging ramps are monitored by

$$-\frac{ESA_\ell^{max}}{\tau_\ell} \leq ESA_\ell^k - ESA_\ell^{k-1} \leq \frac{ESA_\ell^{max}}{\tau_\ell} \tag{17}$$

where $\ell = 1, \ldots, nsd$.

Objective Function

The optimization criterion used in the LMOPF is presented in Equation (1), which is equivalent to the daily operating cost of the system:

$$FO = DailyCost_{withoutStorage}. \tag{18}$$

The optimization problem represented in Equations (6) to (18) was solved using an interior point method with the Linprog function of Matlab®.

RESULTS

The network system considered in the present work for simulations and analyses is part of the southern Brazilian system, and consists of 408 buses, 615 high voltage lines, 26 HPPs (of which 10 could be allocated to daily cycle PHESs), four TPPs, and two wind farms (WFs). The viable sets for the allocation of BESSs, LAESs and GESSs were the same as each other, and were formed of 230 kV buses. The number of ESSs to allocate was 12.

Two different cases were considered for the MCs: high MC and low MC, corresponding to values verified during the dry and wet seasons, respectively, of the year 2021 [36]. However, the model does not depend on these input variables, and other non-zero values could be chosen. Each MC case was divided into three load periods: low, medium, and high. The values of these input variables are presented in Table 8.

Table 8. Values and levels of MC

Item	Low Level	Medium Level	High Level
Level period	01:00 to 07:00 h	08:00 to 18:00 h and 22:00 to 24:00 h	19:00 to 21:00 h
Level duration	7 hours	14 hours	3 hours
High MC ($/MWh)	572.50	590.70	593.00
Low MC ($/MWh)	34.35	36.00	36.20

Two cases of allocations were considered: with and without allocations. This gave a total of four cases for analysis, from the combination of MC values and allocations possibilities, as shown in Table 9.

Table 9. Cases analyzed

Allocations	Low MC	High MC
Without	Case A-0	Case B-0
With	Case A	Case B

Five simulations were carried out for each case. The results of specific simulations (called the “base simulations”) are presented for each case below.

The results for cases without allocations were obtained by setting to zero the number of ESSs to be allocated before executing the optimization model. These results were compared with the results of cases with allocations. Positive results were obtained for cases A and B, indicating that the allocations were viable. Therefore, the net result can be understood as an allocation signal.

Table 10 shows the computational and allocation results, Table 11 shows the financial results, and Table 12 shows the energy results for the cases analyzed. The base power is 100 MVA.

Table 10. Computational and allocation results

Item	Case A-0	Case A	Case B-0	Case B
Fitness	6.8287e+07	6.8013e+07	2.6981e+08	2.6796e+08
CPU time (s)	9,765.40	11,161.60	9,765.40	11,161.60
Number of Allocations	–	Seven	–	Eight

Table 11. Financial results (in thousands of dollars

Item	Case A-0	Case A	Case B-0	Case B
ESS daily cost	–	8.95	–	15.75
Total hydro cost	2,609.70	2,605.75	42,914.50	42,520.85
Total thermal cost	5,936.00	5,927.85	5,936.00	5,933.60
Total load shedding cost	5,111.60	5,061.00	5,111.55	5,122.50
Total daily cost	13,657.30	13,602.55	53,962.10	53,592.60
Daily net result	–	54.75	–	369.50

Table 12. Energy results (puh)

Item	Case A-0	Case A	Case B-0	Case B
Total hydro	704.40	704.40	704.40	704.40
Total low-level hydro	109.70	117.70	109.70	125.20
Total medium level hydro	470.34	466.27	470.34	485.00
Total high-level hydro	124.36	120.48	124.36	94.20
Total thermal	5.80	5.79	5.80	5.79
Total wind generation	125.64	125.64	125.64	125.64
Total load shedding	33.44	33.11	33.44	33.50

Results for Cases A-0 and A

It can be observed from Table 11 that the daily net results for Cases A and B were positive. In Case A, the net result was $ 54.75 thousand, mainly due to the reduction in hydroelectric generation from 124.36 puh to 120.48 puh during the high-level period, as shown in Table 12.

Figure 1 shows the curves for the total hourly hydroelectric generation, total hourly thermoelectric generation, total hourly wind generation, and total hourly load shedding for Case A-0 (no allocations). Figure 2 shows these same curves, but for Case A (seven allocations), and also shows the charging and discharging curve for the ESS allocated in this case.

Figure 2 shows that there was a decrease in the hydroelectric generation during the high-level period, when the MC value was high, and an increase during the low-level period, when MC value was low. As a result, the cost of hydroelectric generation decreased after the allocation of the ESS.

Figure 3 shows the same variables as Figure 2, but without the total hydroelectric and thermoelectric generation, so that the differences between the total hourly wind generation, the total hourly load shedding and the total hourly charging and discharging of the ESS can be analyzed with greater precision.

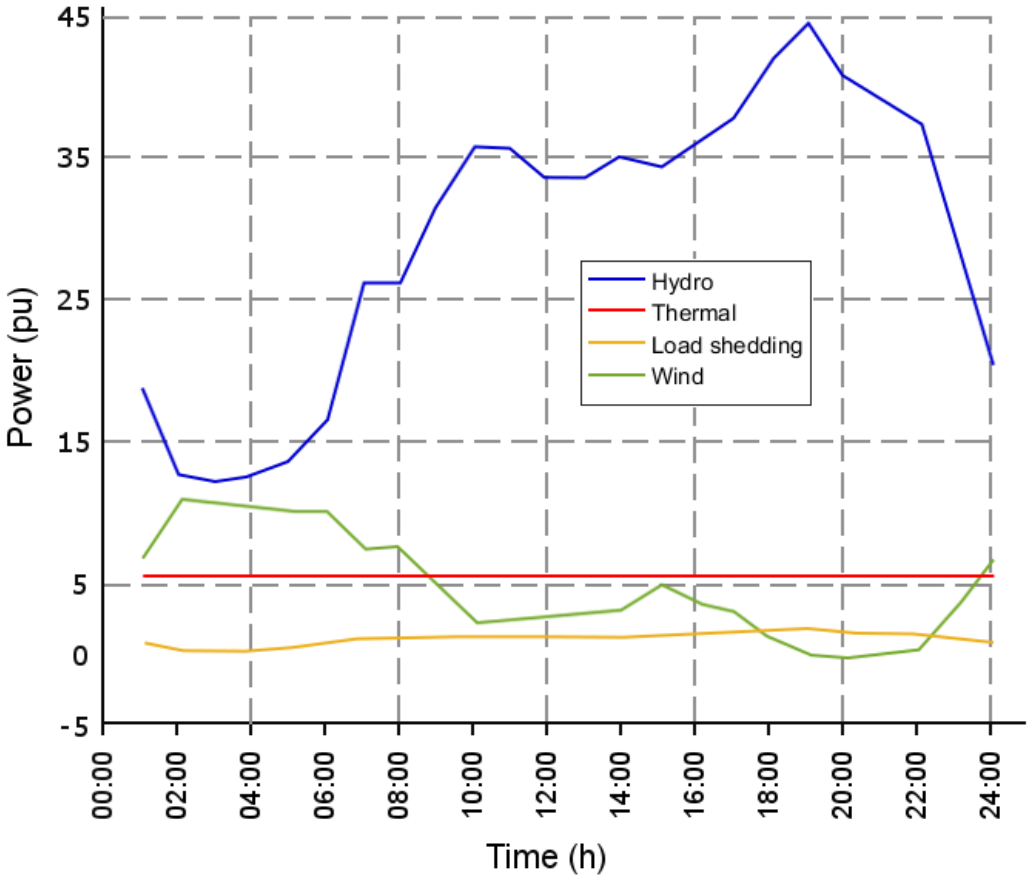

Figure 1. Comparative results for Case A-0

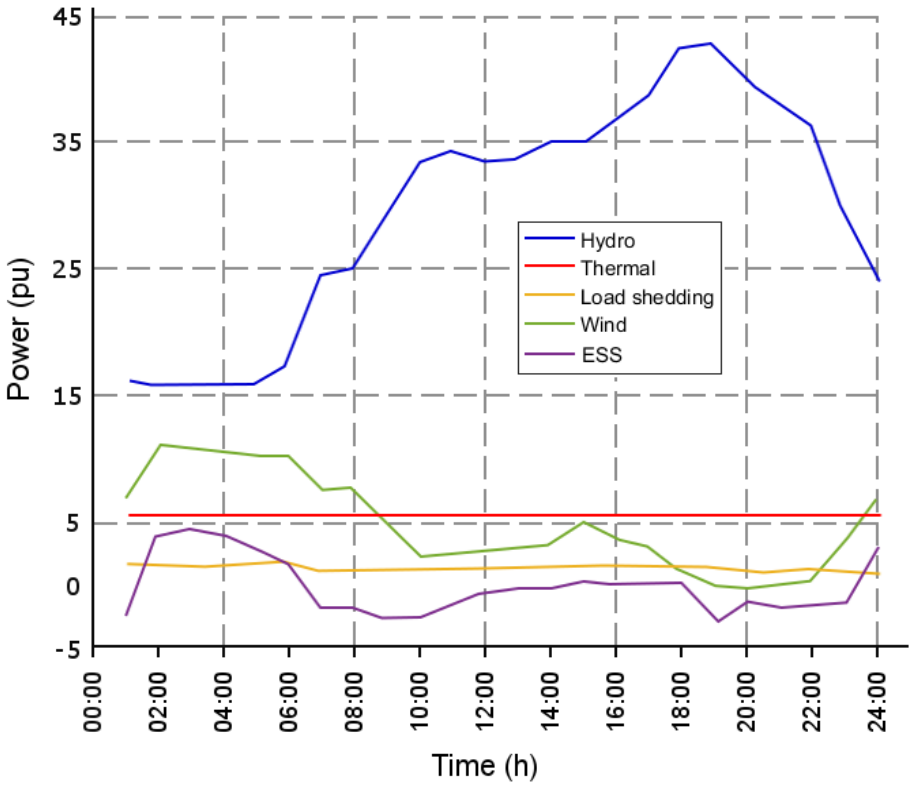

Figure 2. Comparative results for Case A

It can be observed from Figure 3 that the ESS is charging between 1:00 and 4:00 h, when the MC value is low, and the wind generation is high. It can also be observed that the ESS is discharging between 4:00 and 10:00 h, when the MC value is medium, and when the wind generation is decreasing. The ESS is also charging between 10:00 and 12:00 h and discharging between 18:00 and 21:00 h.

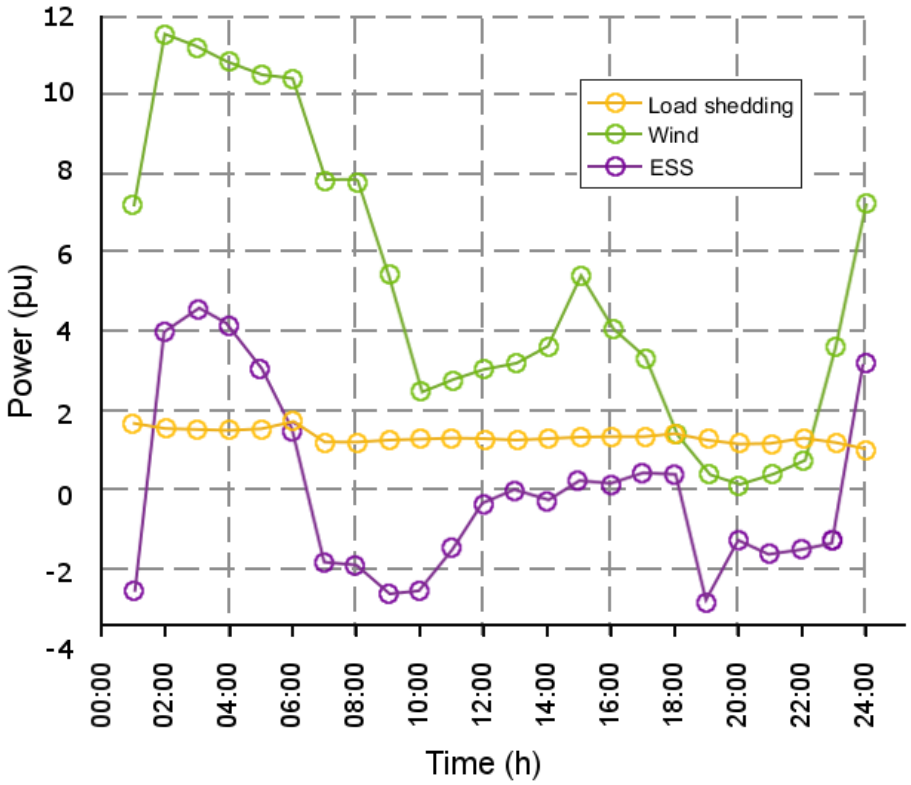

Figure 3. ESS power, wind power, and load shedding for Case A

Results for Cases B-0 and B

It can be observed from Table 12 that the total hydroelectric generation during the high-level period decreased from 124.36 puh to 94.20 puh for Case B. This difference was shifted to the low and medium level periods, where the MC values are lower. Table 11 shows that the net result for Case B was equal to $ 369.50 thousand.

The net result for Case B was higher than the net result for Case A, because the shift value for Case B was higher than the shift value for Case A.

Figure 4 shows the curves for the total hourly hydroelectric, thermoelectric and wind generation, and the curve for the total hourly load shedding for Case B-0 (no allocations). Figure 5 shows these same curves, but for Case B (eight allocations), and also shows the charging and discharging curve for the ESS allocated in this case.

Figure 6 shows the same variables as Figure 5, but without the total hydroelectric and thermoelectric generation, so that the differences between the total hourly wind generation, the total hourly load shedding and the total hourly charging and discharging of the ESS can be analyzed with greater precision.

It can be observed from Figure 6 that the ESS is charging between 1:00 and 4:00 h, when the MC value is low, and the wind generation is high. It can also be observed that the ESS is discharging between 4:00 and 10:00 h, when the MC value is medium, and when the wind generation is decreasing. The ESS is also charging between 10:00 and 18:00 h and discharging between 18:00 and 21:00 h. In this case the high MC value at the high-level period allows for a high discharge of the ESS. The charging and discharging processes for Case A (Figure 3) and for Case B (Figure 6) are similar. However, this process is more intense for Case B than for Case A, due to the higher MC values of Case B (Table 8).

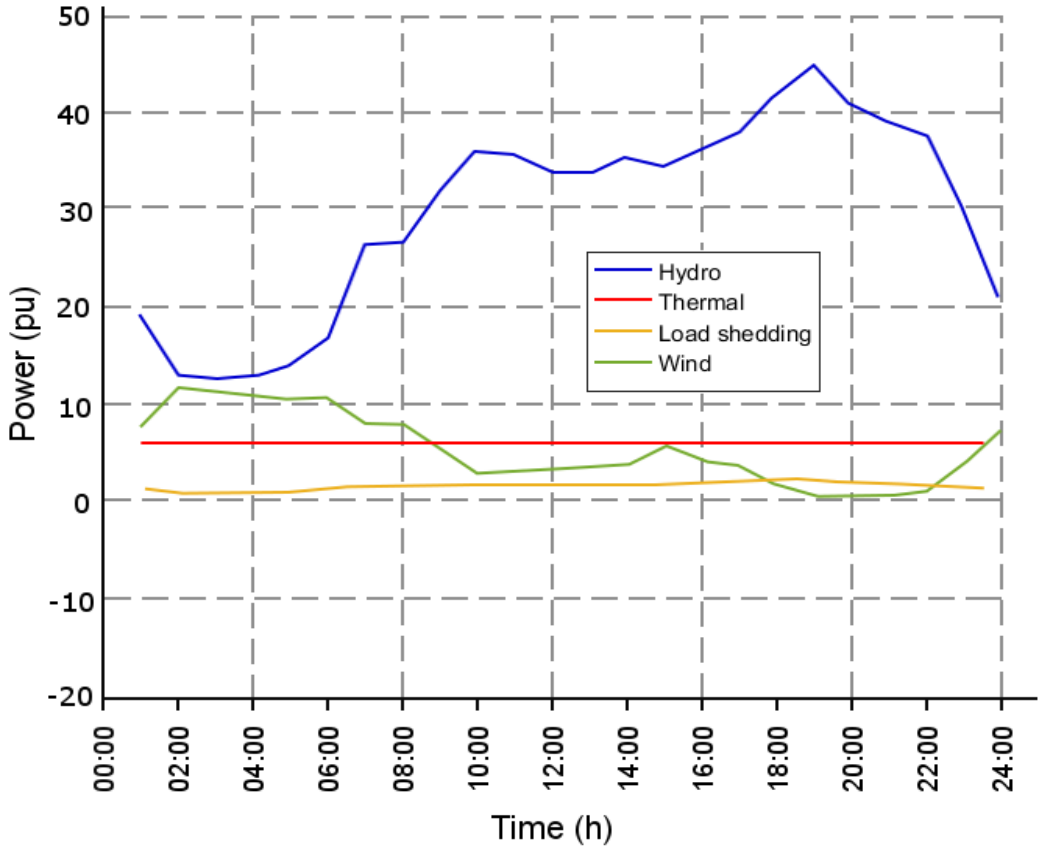

Figure 4. Comparative results for Case B-0

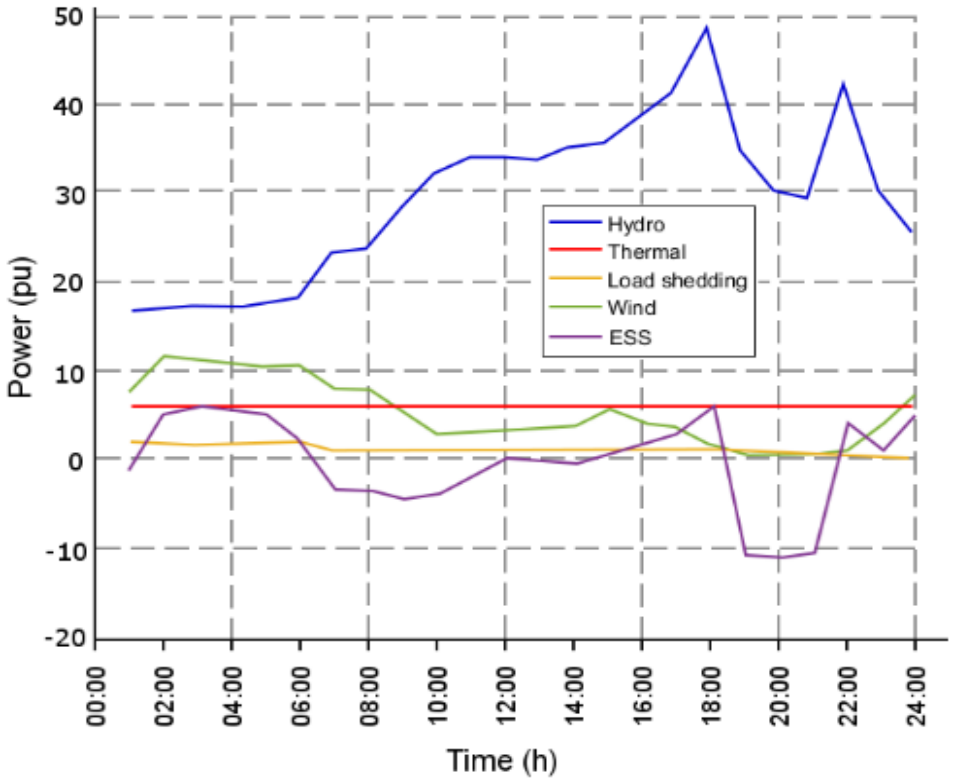

Figure 5. Comparative results for Case B

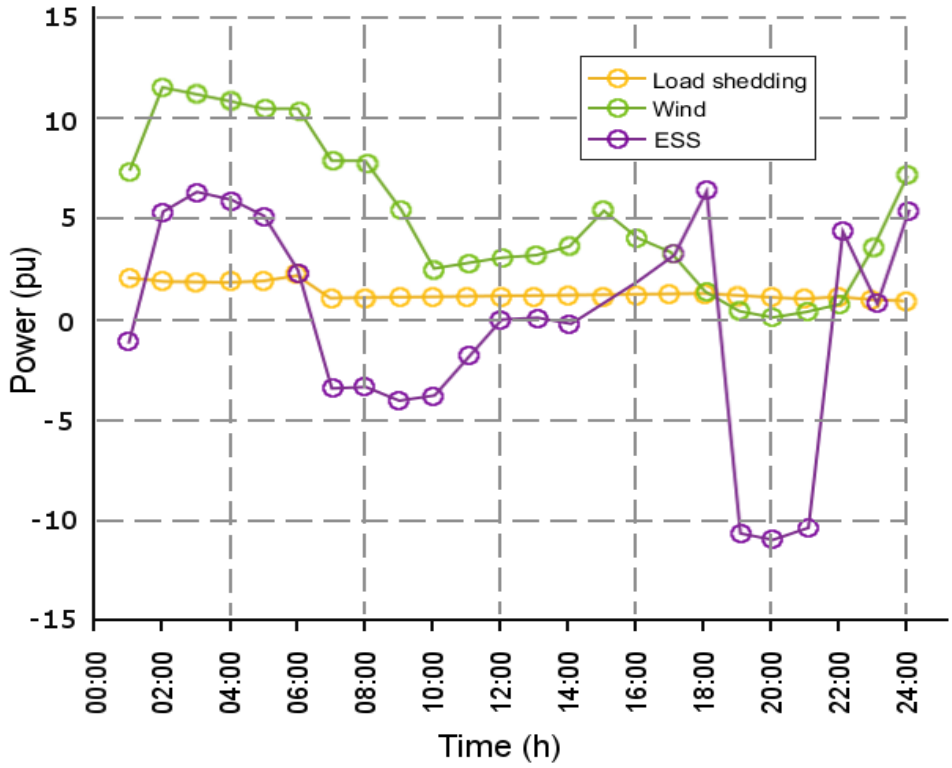

Figure 6. ESS power, wind power, and load shedding for Case B

Tables 13 and 14 show the buses where the ESSs were allocated in the base simulations of Cases A and B, respectively. It can be observed that the largest ESS allocated were always a BESS, and that most of them were allocated to the largest load centers in Paraná (PR). The exception was the BESS allocated to bus 145, Dourados, Mato Grosso do Sul (MS).

BESS was the most frequently allocated type of ESS technology, despite their reduced lifetime. The other parameters (low cost and high cycle efficiency) outweigh their lifetime.

Table 13. Allocations for Case A (Base Sim)

Bus No	Bus name	Type of ESS	Size (MW/MWh)
26	Bateias, PR	GESS	20/100
51	Cascavel, PR	BESS	800/1200
55	Figueira, PR	BESS	20/100
145	Dourados, MS	BESS	100/400
243	Cascavel Oeste, PR	GESS	20/100
323	Curitiba, PR	GESS	20/100
377	Cascavel Norte, PR	GESS	20/100

Table 14. Allocations for Case B (Base Sim)

Bus No	Bus name	Type of ESS	Size (MW/MWh)
26	Bateias, PR	BESS	200/800
30	São José dos Pinhais, PR	GESS	20/100
89	Apucarana, PR	BESS	800/1200
121	Campo Mourão, PR	LAES	50/200
125	Guaira, PR	BESS	20/100
172	Rio Branco, PR	BESS	800/1200
213	São Mateus, PR	BESS	20/100
318	Curitiba, PR	BESS	500/1000

Results for other simulations

Five simulations were carried out for each case. Due to the size of the system and the stochasticity of the model, the GA found different allocation solutions for different simulations.

Tables 15 and 16 show the allocation results for all simulations of cases A and B, respectively. The following conclusions can be drawn from these simulations:

- BESSs were allocated in 4 simulations of Case A, and in all simulations of Case B. This is also the case of GESSs;
- LAESs were allocated only in one simulation of Case A, and in two simulations of Case B;
- PHESs were allocated in 3 simulations of Case A, but not for the base simulation of this case.
- PHESs were not allocated in any simulation of Case B.

Table 15. Types and numbers of allocated ESS: simulations of Case A

Type of ESS	Base Sim	Sim 1	Sim 2	Sim 3	Sim 4
PHES	0	1	1	0	1
BESS	3	3	5	0	3
LAES	0	1	0	0	0
GESS	4	3	0	6	3
Total	7	8	6	6	7

Table 16. Types and numbers of allocated ESS: simulations of Case B

Type of ESS	Base Sim	Sim 1	Sim 2	Sim 3	Sim 4
PHES	0	0	0	0	0
BESS	6	6	4	6	4
LAES	1	0	0	1	0
GESS	1	2	4	1	2
Total	8	8	8	8	6

Table 17 and Table 18 show a summary of the numeric results obtained for all simulations of Case B (which was chosen for illustrated in more detail). There were positive net results for all simulations of Case B. Moreover, the energy time-shift was similar for all simulations. It can be observed that the highest daily

net result occurred for Sim 2 ($ 387.00 thousand). This simulation also presented the lowest hydrogeneration at the high-level period (92.34 puh). Thus, higher energy time-shift allows for higher daily net results.

Comparative curves, such as those in Figure 2 and Figure 5, could be drawn for the other simulations to demonstrate this behavior. There were also positive net results for all simulations of Case A, but they were not shown in this paper, due to space restrictions.

Table 17. Financial results for all simulations of Case B (in thousands of dollars)

Item	Base Sim	Sim 1	Sim 2	Sim 3	Sim 4	Average value	Standard deviation
ESS daily cost	15.75	13.20	15.16	15.75	13.61	14.70	1.21
Total hydro cost	42,520.85	42,541.20	42,496.80	42,520.90	42,533.60	42,522.67	16.87
Total thermal cost	5,933.60	5,931.80	5,933.80	5,933.60	5,933.80	5,933.32	0.86
Total load shedding cost	5,122.50	5,132.70	5,129.30	5,122.40	5,130.30	5,126.13	4.26
Total daily cost	53,592.60	53,620.80	53,575.00	53,592.60	53,611.30	53,592.88	14.82
Daily net result	369.50	342.30	387.00	369.50	350.80	369.20	14.78

Table 18. Energy results for all simulations of Case B (puh)

Item	Base Sim	Sim 1	Sim 2	Sim 3	Sim 4	Average value	Standard deviation
Total hydro	704.40	704.40	704.40	704.40	704.40	704.40	0.00
Total low-level hydro	125.19	123.39	126.27	125.19	123.88	124.78	1.15
Total medium level hydro	485.05	485.44	485.78	485.05	485.50	485.36	0.32
Total high-level hydro	94.16	95.57	92.34	94.16	95.02	94.25	1.22
Total thermal generation	5.80	5.80	5.80	5.80	5.80	5.80	0.00
Total wind generation	125.64	123.84	123.84	123.84	123.84	124.20	0.80
Total load shedding	33.51	33.57	33.55	33.51	33.56	33.54	0.03

CONCLUSION

This work has proposed a model for the optimal allocation of ESS in HV hydro-thermal-wind systems. The allocation considered four ESS technologies: PHES, BESS, LAES and GESS, each one with different parameters. The linear optimization problem was resolved using a genetic algorithm (GA) and a linear multi-period optimal power flow (LMOPF).

Four cases were defined to test the model: high MC and low MC, each one divided into cases with and without allocations. The results for cases with allocations were compared with those without allocations. Positive results were obtained, indicating that allocations were viable.

Five simulations were carried out for each case, and the results showed that the model operates satisfactorily. This is an important contribution of the present work.

BESSs were allocated in many simulations, due to their low cost and high cycle efficiency, despite their reduced lifetime. Moreover, the results for the base simulations of Cases A and B indicate that the largest ESS was always a BESS. GESSs were also allocated in many simulations. However, in the base case, they had always the lowest size (20 MW/100 MWh).

LAESs were allocated in few simulations compared to BESSs and to GESSs. This could be expected, due to their high cost and low cycle efficiency, despite their long lifetime. This is also the case of PHESs. An additional restriction for the allocation of PHESs was the bus availability: there were only 10 ESSs of this type of technology in the system.

The allocation results for different ESS technologies in different cases indicated that costs, cycle efficiencies, and available buses are the most important parameters. The other parameters (lifetimes, discharge times, and power ranges), play secondary roles. This is another important contribution of the present work.

There was a tendency to charge the ESSs during the low-level period, when the MC value was low, and the wind power was high. There was also a tendency to discharge the ESSs during the medium level period, when the MC value was medium, and the wind power was decreasing. The highest discharge occurred during the high-level period, when the MC value was high, and the wind power was zero.

The total hydroelectric generation was the same for all cases and simulations (704,40 puh), with and without allocations. However, the hydroelectric energy was always shifted to the other levels when the ESSs were allocated, initiating a charging and discharging process, reducing the hydroelectric energy at the high level, and resulting in positive net results.

Acknowledgements: The authors thank CAPES—Brazilian Federal Agency for Support and Evaluation of Graduate Education the Ministry of Education of Brazil, Federal University of Parana (UFPR) and Federal University of Technology-Parana (UTFPR).
Conflicts of Interest: The authors declare no conflict of interest.

REFERENCES

1. Fearnside PM. Impacts of Brazil's Madeira River Dams: Unlearned lessons for hydroelectric development in Amazonia. Environ Sci Policy. 2014; (38): 164–72.
2. Proser N. Energy Storage: Technology for a More Efficient Grid. Senior Thesis. Claremoint Colleges; 2011.
3. Eyer J, Corey G. Energy Storage for the Electricity Grid: Benefits and Market Potential Assessment Guide A Study for the DOE Energy Storage Systems Program [Internet]. Oak Ridge: DOE; 2010. Available from: https://www.sandia.gov/ess-ssl/publications/SAND2010-0815.pdf.
4. Bradbury K, Pratson L, Patiño-Echeverri D. Economic viability of energy storage systems based on price arbitrage potential in real-time U.S. electricity markets. Appl Energy. 2014; (114): 512–9.
5. Staffell I, Rustomji M. Maximising the value of electricity storage. J Energy Storage. 2016; (8): 212–25.
6. US Department of Energy. Potential benefits of High-Power High-Capacity BESS. [cited 2024 Jan 2]; Available from: https://www.energy.gov/oe/articles/potential-benefits-high-power-high-capacity-batteries-january-2020.
7. Aneke M, Wang M. Energy storage technologies and real-life applications – A state of the art review. Appl Energy. 2016; (179): 350–77.
8. Awad ASA, El-Fouly THM, Salama MMA. Optimal ESS allocation and load shedding for improving distribution system reliability. IEEE Trans Smart Grid. 2014; (5) :2339–49.
9. Babacan O, Torre W, Kleissl J. Optimal allocation of battery energy storage systems in distribution networks considering high PV penetration. In: IEEE Power and Energy Society General Meeting. IEEE Computer Society; 2016.
10. Awad ASA, EL-Fouly THM, Salama MMA. Optimal ESS Allocation for Benefit Maximization in Distribution Networks. IEEE Trans Smart Grid. 2017; (8):1668–78.
11. Rangel CAS, Canha L, Sperandio M, Severiano R. Methodology for ESS-type selection and optimal energy management in distribution system with DG considering reverse flow limitations and cost penalties. IET Generation, Transmission and Distribution. 2018; (12):1164–70.
12. Mazza A, Mirtaheri H, Chicco G, Russo A, Fantino M. Location and sizing of battery energy storage units in low voltage distribution networks. Energies. 2019; (13).
13. Wong LA, Ramachandaramurthy VK. Optimal allocation of battery energy storage system using whale optimization algorithm. In: International Conference on Electrical, Computer, Communications and Mechatronics Engineering, ICEC-CME 2021. Institute of Electrical and Electronics Engineers Inc.; 2021.
14. DOE 2023 [cited 2023 Jul 21]. DOE Global Energy Storage Database. Available from: https://gesdb.sandia.gov/
15. Brandão R, Nivalde DC, Hunt J. [The Viability of Reversible Power Plants in the National Interconnected System (GESEL) – UFRJ]; 2021 [cited 2021 Dec 29]. Available from: https://www.projetouhr.com.br/livro.php.
16. Energy Research Office. [Inventory study of Reversible Hydroelectric Power Plants (UHR): Methodology and preliminary results for the State of Rio de Janeiro] [Internet]. 2019 [cited 2019 Jun 27]. Available from: https://www.epe.gov.br/sites-pt/publicacoes-dados-abertos/publicacoes/PublicacoesArquivos/publicacao-353/EPE-DEE-NT-006_2019-r0.pdf.
17. Edge JS, O'Kane S, Prosser R, Kirkaldy ND, Patel AN, Hales A, et al. Lithium-ion battery degradation: What you need to know. Physical Chemistry Chemical Physics. 2021, (23): 8200–21.
18. Colthorpe A. Energy Storage. 2023 [cited 2024 Jan 19]. Moss Landing: World's biggest battery storage project is now 3GWh capacity. Available from: https://www.energy-storage.news/moss-landing-worlds-biggest-battery-storage-project-is-now-3gwh-capacity.
19. Queiroz K, Saar S. ISA CTEEP, [ANEEL and MME inaugurate Brazil's first large-scale energy storage Project] [Internet]. 2023 [cited 2023 Nov 4]. Available from: https://www.isacteep.com.br/pt/noticias/isa-cteep-aneel-e-mme-inauguram-primeiro-projeto-de-armazenamento-de-energia-em-larga-escala-do-brasil.
20. Energy Research Office (Empresa de Pesquisa Energética, EPE). [Battery Storage Systems: Applications and issues relevant to planning] [Internet]. 2019. [cited 2019 Jun 27]. Available from: https://www.epe.gov.br/pt/publicacoes-dados-abertos/publicacoes/nt-sistemas-de-armazenamento-em-baterias-aplicacoes-e-questoes-relevantes-para-o-planejamento.
21. Oening AP, Marcilio DC, Andrade J, Impinnisi PR. Analytic hierarchy process algorithm applied to Battery Energy Storage System selection for Grid Applications. Brazilian Archives of Biology and Technology. 2021; 64(spe).
22. Vecchi A, Li Y, Ding Y, Mancarella P, Sciacovelli A. Liquid Air Energy Storage (LAES): A review on technology state-of-the-art, integration pathways and future perspectives. Advances in Applied Energy. Elsevier; 2021; (3).

23. Highview Power [Internet]. 2018 [cited 2018 Aug 9]. Available from: https://www.highviewpower.com.
24. Tong W, Lu Z, Chen W, Han M, Zhao G, Wang X, et al. Solid gravity energy storage: A review. J Energy Storage. 2022; (53).
25. Botha CD, Kamper MJ. Capability study of dry gravity energy storage. J Energy Storage. 2019; (23): 159–74.
26. Energy Vault [Internet]. 2021 [cited 2021 Dec 28]. Available from: https://www.energyvault.com/project-cn-rudong.
27. Moore S. The Ups and Downs of Gravity Energy Storage: Startups are pioneering a radical new alternative to batteries for grid storage. IEEE Spectrum. 2021; (58): 38–9.
28. Awad ASA, El-Fouly THM, Salama MMA. Optimal ESS allocation and load shedding for improving distribution system reliability. IEEE Trans Smart Grid. 2014; (5): 2339–49. (7)
29. Zhang Z, Ding T, Zhou Q, Sun Y, Qu M, Zeng Z, et al. A review of technologies and applications on versatile energy storage systems. Renew. Sust. Energ. Rev. 2021; (148). (26)
30. Kebede AA, Kalogiannis T, Van Mierlo J, Berecibar M. A comprehensive review of stationary energy storage devices for large scale renewable energy sources grid integration. Renew. Sust. Energ. Rev. 2022; (159).
31. Mitali J, Dhinakaran S, Mohamad AA. Energy Storage Systems: A review. Energy Storage and Saving. 2022; (1): 166–216.
32. Benchmark Source. Global cell prices fall below $100/kWh for first time in two years. Benchmark Source [Internet]. 2023 [cited 2024 Jan 1]; Available from: https://source.benchmarkminerals.com/article/global-cell-prices-fall-below-100-kwh-for-first-time-in-two-years.
33. Liang T, Zhang T, Lin X, Alessio T, Legrand M, He X, et al. Liquid Air Energy Storage technology: A comprehensive review of research, development and deployment. Progress in Energy. 2023; (5).
34. Blasi TM, Fernandes TSP, Aoki AR, Tabarro FH. Multiperiod optimum power flow for active distribution networks with provisioning of ancillary services. IEEE Access. 2021; (9): 110371–95.
35. Coello CAC. An updated survey of GA-based multiobjective optimization techniques. ACM Computing Surveys, 2000; (32): 109–43.
36. National Electric System Operator. [cited 2023 Jul 31]. [Marginal Operating Cost] (CMO). Available from: https://www.ons.org.br/Paginas/resultados-da-operacao/historico-da-operacao/cmo.aspx.